Reconstruction of radar waveforms with spectral gaps using an autoregressive model

S D Hayward

QinetiQ Ltd, Malvern Technology Centre, St Andrews Road, Malvern, UK

Abstract

This paper describes a computationally efficient method for reconstructing radar signals where samples are missing at the receiver due to sparse spectral sampling. This problem may arise in practice from the need to avoid bands containing interfering signals or to reduce the time required to transmit a stepped-frequency waveform. Without mitigation the missing frequency samples lead to high range sidelobes following pulse compression, making it difficult to detect small targets close to large targets. Examples are provided showing that range sidelobes are significantly reduced when the waveforms are compressed following reconstruction using an autoregressive model.

1. Context

The military utility of imaging radars is well known for target detection and identification using Synthetic Aperture Radar (SAR) techniques. A particular example of this is Low Frequency (LF) SAR, which exploits the penetrative properties of transmissions at longer wavelengths to form images of targets otherwise concealed by foliage or under camouflage.

A major problem with LF SAR systems is that they operate in the crowded VHF/UHF radio frequency bands, suffering interference from the large number of television, radio and communications transmitters, and unable to transmit on other frequencies because of the need to avoid mutual interference. The result is that the echo signals received by the radar are full of spectral gaps. These gaps distort the image formation process and introduce artefacts into the resulting imagery. See for example Lamont-Smith et al. (2006).

Many radar systems require high range resolution in order to discriminate between targets and background clutter (e.g. ground penetrating radar) or to support target identification (e.g. air-to-air radar). The use of stepped-frequency waveforms is common in such systems, since these provide a wide effective bandwidth, while requiring only a narrow instantaneous bandwidth, which makes receiver design easier and reduces costs. In a stepped-frequency radar multiple narrow-band pulses are transmitted, with the centre frequency of each pulse increasing by a fixed step relative to the pulse transmitted previously. By transmitting at a sparse set of frequencies radar resolution is maintained, but the operating time required can be significantly reduced, increasing the responsiveness of the radar to a dynamic environment. Unless corrections are applied the resulting spectral gaps will corrupt the resulting range profiles.

2. Problem

The process of radar scattering from a complex target is illustrated in Figure 1, where returns from two distinct scattering centres are depicted. High Range Resolution (HRR) profiles are obtained by pulse compression in the “frequency direction” which is achieved by applying a matched filter corresponding to an inverse discrete Fourier transform.

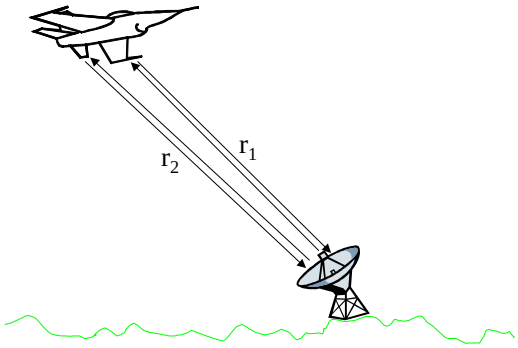

Figure 1: Illustration of a basic range profiling scenario

Figure 2 shows HRR profiles corresponding to a simulated target comprising five point scatterers with random phases and a 30dB amplitude range. A 30dB Chebyshev window has been applied to suppress range sidelobes. A stepped frequency waveform with 128 steps is used to create the original HRR profile, in which all five scatterers are visible. When half of the frequency steps are omitted, following the binary mask pattern shown in Figure 3, sidelobes from the two strongest scatterers rise to around 20dB and obscure the three weaker scatterers.

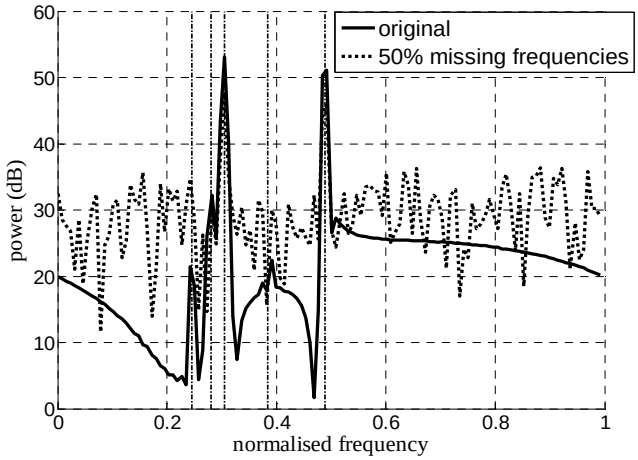

Figure 2: Simulated HRR profile from a target with five point scattering centres

Figure 3: Sampling within the set of 128 frequency steps with missing samples shown in white.

3. Solution

There are several possible solutions to this problem. Pulse compression repair algorithms, which aim to recover a low range sidelobe solution using a minimum mean square error criterion, are described in Lane (2006). A compressive sensing approach has been developed in Kelly et al. (2011), in which a SAR image is reconstructed from the phase history data through the iterative solution of a regularised least squares minimisation problem. Regularisation of the solution is achieved through addition of a term which controls the level of sparsity in the reconstructed image.

Both these approaches are known to have a high computational load, involving iterative calculations, requiring $\mathcal{O}(N^2 log N)$ operations per iteration, where N is the number of

frequency steps in the HRR profiling problem or the number of pulses (assumed equal to the number of samples per pulse) in the SAR image reconstruction problem.

A much more computationally efficient approach is to fit an Autoregressive (AR) model to the measurements and use the model to estimate the missing data through a process of linear "bandwidth interpolation". This method is closely related to so-called super-resolution spectral estimation, which can be thought of as "bandwidth extrapolation", as indicated in Figure 4.

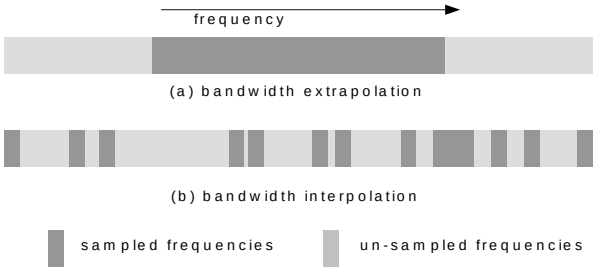

Figure 4: Sampling schemes employed in (a) bandwidth extrapolation and (b) bandwidth interpolation

An AR random process is one whose time series satisfies $a_0^* y(k) = \sum_{i=1}^{p} a_i^* y(k-i) + v(k)$, where p is the model order, $a_0, a_1, \ldots, a_p$ are constants called the AR coefficients, and $\{v(k)\}$ is a white noise process. The first AR coefficient $a_0 = 1$.

The use of an AR model for linear prediction is well known, e.g. Etter (1996). Given an AR sequence of length n in the form of a column vector $\mathbf{y} = [y(1) \quad y(2) \quad \ldots \quad y(n)]^T$, then $\mathbf{e}_f$, the vector of forward prediction errors is related to $\mathbf{y}$ via

$$\mathbf{e}_f = \mathbf{A}_f \mathbf{y}, \tag{3.1}$$

where the matrix $\mathbf{A}_f \in \mathbb{C}^{n \times n}$ is Toeplitz with the first row taking the form $[\mathbf{a}^T \mathbf{0}_{n-p-1}^T]$. Here $\mathbf{a}$ is the column vector containing the $p+1$ AR coefficients, and $\mathbf{0}_k^T$ is the k dimensional null vector. A similar expression can be obtained for $\mathbf{e}_b$, the vector of backward prediction errors,

$$\mathbf{e}_b = \mathbf{A}_b \mathbf{y}, \tag{3.2}$$

where the matrix $\mathbf{A}_b = \mathbf{A}_f^H$, when $\mathbf{e}_b$ is ordered appropriately.

AR extrapolation

When $\mathbf{y}$ contains missing samples, these samples can be estimated using (3.1) and (3.2) to minimise the sum of the squared prediction errors, using either forwards, backwards or a combined prediction error. To see how an AR extrapolation estimate is obtained let the AR sequence represented by $\mathbf{y}$ be partitioned into two sub-sequences, represented by $\mathbf{y} = \begin{bmatrix} \mathbf{y}^1 \\ \mathbf{y}^2 \end{bmatrix}$, where $\mathbf{y}^1 \in \mathbb{C}^{n_1 \times 1}$ contains n_1 *unobserved* samples at the end of the sequence, and $\mathbf{y}^2 \in \mathbb{C}^{n_2 \times 1}$ contains n_2 *observed* samples at the beginning of the sequence. The object of the exercise is to estimate the unobserved samples from those that have been observed, assuming that the AR coefficients, and hence the matrices $\mathbf{A}_b$ and $\mathbf{A}_f$, are known. We can write a partitioned version of (3.1) as

$$\begin{bmatrix} \mathbf{e}_f^1 \\ \mathbf{e}_f^2 \end{bmatrix} = \begin{bmatrix} \mathbf{A}_f^1 & \mathbf{A}_f^2 \\ \mathbf{A}_f^3 & \mathbf{A}_f^4 \end{bmatrix} \begin{bmatrix} \mathbf{y}^1 \\ \mathbf{y}^2 \end{bmatrix}, \tag{3.3}$$

where both $\mathbf{e}_f$ and $\mathbf{A}_f$ have been partitioned such that $\mathbf{e}_f^1 \in \mathbb{C}^{n_1 \times 1}$, $\mathbf{e}_f^2 \in \mathbb{C}^{n_2 \times 1}$, $\mathbf{A}_f^1 \in \mathbb{C}^{n_1 \times n_1}$, $\mathbf{A}_f^2 \in \mathbb{C}^{n_1 \times n_2}$, $\mathbf{A}_f^3 \in \mathbb{C}^{n_2 \times n_1}$, $\mathbf{A}_f^4 \in \mathbb{C}^{n_2 \times n_2}$.

We write the sum of the squared forward prediction errors corresponding to the unobserved samples as $\|\boldsymbol{e}_f^1\|_2^2 = \boldsymbol{e}_f^{1H} \mathbf{e}_f^1 = \left(\mathbf{A}_f^1 \mathbf{y}^1 + \mathbf{A}_f^2 \mathbf{y}^2\right)^H \left(\mathbf{A}_f^1 \mathbf{y}^1 + \mathbf{A}_f^2 \mathbf{y}^2\right)$, and setting the partial derivative with respect to $\mathbf{y}^{1H}$ to zero and solving for $\mathbf{y}^1$ in terms of $\mathbf{y}^2$ yields,

$$\hat{\mathbf{y}}^1 = -\left(\mathbf{A}_f^{1\,H}\mathbf{A}_f^1\right)^{-1}\mathbf{A}_f^{1\,H}\mathbf{A}_f^2\mathbf{y}^2. \tag{3.4}$$

We will refer to this estimator as the forward prediction estimator. The preferred method for solving (3.4) (and subsequent equations with the same structure) is via Cholesky factorisation with computational requirement $\mathcal{O}(n_2p^2)$ due to the banded nature of the matrices involved, and repeated back-substitution. A straightforward extension of (3.4) yields a forwards-backwards least-squares estimator.

From an inspection of (3.3) it is clear that an alternative and apparently new approach to the estimation of the unobserved samples is to make use of the prediction errors corresponding to both the observed and unobserved samples. According to the underlying AR model the prediction errors are white and Gaussian, so by minimising the sum of the squares of all the errors we are maximising the likelihood of the entire sequence of samples. Such an approach might be expected to yield lower estimation errors than one based on the use of the prediction errors of the unobserved samples alone. The pattern of calculation that led to (3.4) is followed in solving for $\mathbf{y}^1$, yielding the following expression

$$\hat{\mathbf{y}}^1 = -\left(\mathbf{A}_f^{1\,H}\mathbf{A}_f^1 + \mathbf{A}_f^{3\,H}\mathbf{A}_f^3 + \mathbf{A}_f^1\mathbf{A}_f^{1\,H} + \mathbf{A}_f^2\mathbf{A}_f^{2\,H}\right)^{-1}\begin{pmatrix}\mathbf{A}_f^{1\,H}\mathbf{A}_f^2 + \mathbf{A}_f^{3\,H}\mathbf{A}_f^4 + \mathbf{A}_f^1\mathbf{A}_f^{3\,H} \\ +\mathbf{A}_f^2\mathbf{A}_f^{4\,H}\end{pmatrix}\mathbf{y}^2. \tag{3.5}$$

We will refer to this estimator as the total forwards and backwards prediction estimator.

AR interpolation

In the previous section it was assumed that both unobserved and observed samples formed a contiguous sequence. Now consider the case where the unobserved samples (or gaps) are randomly distributed throughout the sequence of observed samples, as illustrated in Figure 4(b). Let the complete sequence be represented by the column vector $\mathbf{y}$. An m-dimensional permutation matrix, $\mathbf{P}$, is a matrix obtained by permuting the rows of an identity matrix according to some permutation of the numbers 1 to m. Every row and column therefore contains precisely a single 1 with 0s everywhere else, and every permutation corresponds to a unique permutation matrix. A permutation matrix also satisfies

$$\mathbf{P}\,\mathbf{P}^H = \mathbf{P}^{\boldsymbol{H}}\mathbf{P}=\mathbf{I}. \tag{3.6}$$

There exists a permutation matrix, $\mathbf{P}$, such that the column vector $\tilde{\mathbf{y}} = \mathbf{P}\mathbf{y}$ takes the form $\tilde{\mathbf{y}}=\begin{bmatrix}\tilde{\mathbf{y}}^1\\ \tilde{\mathbf{y}}^2\end{bmatrix}$, where $\tilde{\mathbf{y}}^1 \in \mathbb{C}^{n_1\times 1}$ contains the n_1 unobserved samples, and $\tilde{\mathbf{y}}^2 \in \mathbb{C}^{n_2\times 1}$ contains the n_1 observed samples. It will prove helpful to preserve the order of the samples in $\tilde{\mathbf{y}}^1$ and $\tilde{\mathbf{y}}^2$.

Making use of the property represented in (3.6), we can rewrite (3.1) in terms of a permuted prediction error vector, $\tilde{\boldsymbol{e}}_f$, permuted matrix of autocorrelation coefficients, $\widetilde{\boldsymbol{A}}_{\boldsymbol{f}}$, and a permuted sample vector, $\tilde{\mathbf{y}}$,

$$\tilde{\mathbf{e}}_f \equiv \begin{bmatrix}\tilde{\mathbf{e}}_f^1\\ \tilde{\mathbf{e}}_f^2\end{bmatrix} = \mathbf{P}\begin{bmatrix}\mathbf{e}_f^1\\ \mathbf{e}_f^2\end{bmatrix} = \left(\mathbf{P}\begin{bmatrix}\mathbf{A}_f^1 & \mathbf{A}_f^2\\ \mathbf{A}_f^3 & \mathbf{A}_f^4\end{bmatrix}\mathbf{P}^{\boldsymbol{H}}\right)\left(\mathbf{P}\begin{bmatrix}\mathbf{y}^1\\ \mathbf{y}^2\end{bmatrix}\right) \equiv \begin{bmatrix}\widetilde{\mathbf{A}}_f^1 & \widetilde{\mathbf{A}}_f^2\\ \widetilde{\mathbf{A}}_f^3 & \widetilde{\mathbf{A}}_f^4\end{bmatrix}\begin{bmatrix}\tilde{\mathbf{y}}^1\\ \tilde{\mathbf{y}}^2\end{bmatrix}. \tag{3.7}$$

Because (3.7) has exactly the same structure as (3.3), and there is a permuted equivalent for expressions involving $\mathbf{e}_b$, all the estimators derived above are effective when evaluated using the permuted quantities.

Once an estimate for $\tilde{\mathbf{y}}^1$ is obtained, the original permutation is inverted to recover an estimate of the original sample sequence, $\hat{\mathbf{y}}=\mathbf{P}^H\begin{bmatrix}\tilde{\mathbf{y}}^1\\ \tilde{\mathbf{y}}^2\end{bmatrix}$.

The remaining problem is how to obtain good estimates of the AR coefficients from sparsely sampled data. To do this we have developed an iterative scheme, based on the following two steps. In the first step, given an estimate of the AR coefficients, $\hat{\mathbf{a}}_i$, an estimate

of the complete data sequence, $\hat{\mathbf{y}}_i$, can be obtained using the methods described in the previous section.

In the second step $\hat{\mathbf{y}}_i$ is used to compute $\hat{\mathbf{a}}_{i+1}$, using the Burg algorithm (Marple 1987). The process is repeated until convergence i.e. $\left\|\hat{\mathbf{a}}_{i+1} - \hat{\mathbf{a}}_i\right\|_2^2 \leq t$, where t is a user-defined threshold value. In order to start the process, $\hat{\mathbf{a}}_0$, an initial estimate of the AR coefficients is required. The Levinson-Durbin recursion (Marple 1987) can be used to estimate the AR coefficients from the first $p+1$ samples of the autocorrelation sequence. These samples can be estimated from the data providing that the sampling pattern is 'fully augmentable', in the terminology of Abramovich et al. (1996). This is not a particularly restrictive requirement, and accommodates very sparse sampling schemes.

This iterative approach has been found to converge rapidly and consistently in practice. Because the Burg algorithm chooses its estimates of the AR coefficients to minimise the sum of squared forward and backward prediction residuals, the iterative process described above can be thought of as an example of an alternating minimisation algorithm. The sequences $\{\hat{\mathbf{y}}_i\}$ and $\{\hat{\mathbf{a}}_i\}$ can be shown to converge locally, under some mild assumptions (see for example Byrne 2011).

4. Examples

To illustrate the efficacy of the proposed approach the data used to produce the example HRR profile shown in Figure 2 has been processed using a 5th order AR model. After 10 iterations we get the results shown in Figure 5. The low-sidelobe structure of the original HRR profile has been largely recovered.

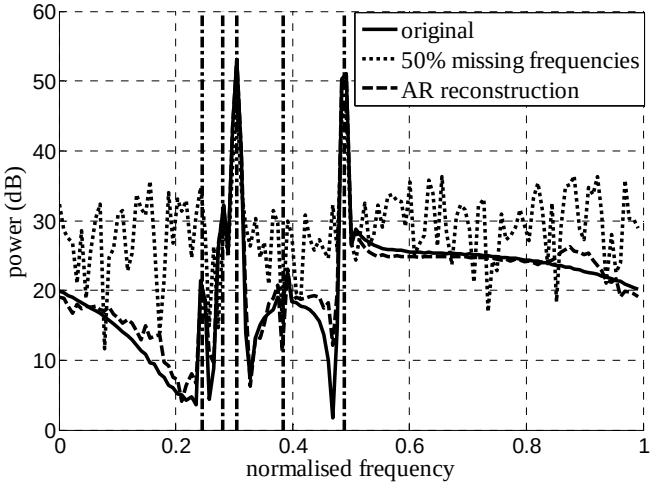

Figure 5: Simulated HRR profile from a target with five point scattering centres showing AR reconstruction using 50% of the frequency samples.

Figure 6 shows range responses extracted from SAR imagery generated from measured LF data. A fence crossing the scene forms a bright target centred in range at the 220th pixel and it is clear that the AR reconstruction algorithm using a model order of 84 has been successful in reducing the sidelobes by up to 6dB. This will improve the sensitivity of the system to weak targets.

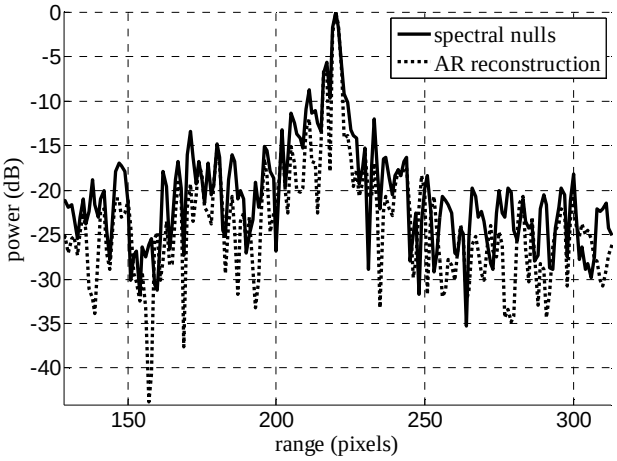

Figure 6: Measured range profiles extracted from LF SAR imagery showing the response to a straight wire fence before and after waveform reconstruction.

5. Summary

A new approach has been described for mitigating the presence of spectral gaps in data used in imaging radar systems, although a similar idea applied to spectrum analysis is described in Fahlman & Ulrych (1982). The use of an AR model for the data is found to be more efficient computationally than alternative methods and has been demonstrated to be effective in reducing the impact of artefacts induced by spectral gaps in real radar data.

ACKNOWLEDGMENT

This work was carried out as part of the MoD Research Programme.

REFERENCES

LAMONT-SMITH, T., HILL, R. D., HAYWARD S. D., YATES, G. & BLAKE, A. 2006. Filtering approaches for interference suppression in low-frequency SAR, IEE Proc Radar Sonar Navig, 153(4):338-344.

LANE, R.O. 2006. The effects of Doppler and pulse eclipsing on sidelobe reduction techniques, IEEE Conference on Radar, 24-27 April 2006, pp.776-781.

KELLY, S. I., RILLING, G., DAVIES, M. MULGREW, B. 2011. Iterative image formation using fast (Re/Back)-projection for spotlight-mode SAR, IEEE Radar Conference (RADAR 2011), pp.835-840.

ETTER, W. 1996. Restoration of a discrete-time signal segment by interpolation based on the left-sided and right-sided autoregressive parameters, IEEE Transactions on Signal Processing, 44(5):1124 - 1135.

ABRAMOVICH, Y. I. et al. 1996. Positive Definite Toeplitz, Completion in DOA Estimation for Fully Augmentable Non-uniform Linear Antenna Arrays, Proceedings of the 1996 IEEE Conference on Acoustics Speech and Signal Processing, 5:2551-2554.

MARPLE, S. L., JR. 1987. Digital Spectral Analysis with Applications, Prentice-Hall.

BYRNE, C. L. 2011. Alternating Minimization and Alternating Projection Algorithms: A Tutorial, Sciences New York, pp.1-41.

FAHLMAN, G. G. & ULRYCH, T. J. 1982. A New Method for Estimating the Power Spectrum of Gapped Data, Monthly Notices of the Royal Astronomical Society, 199(1):53-65.